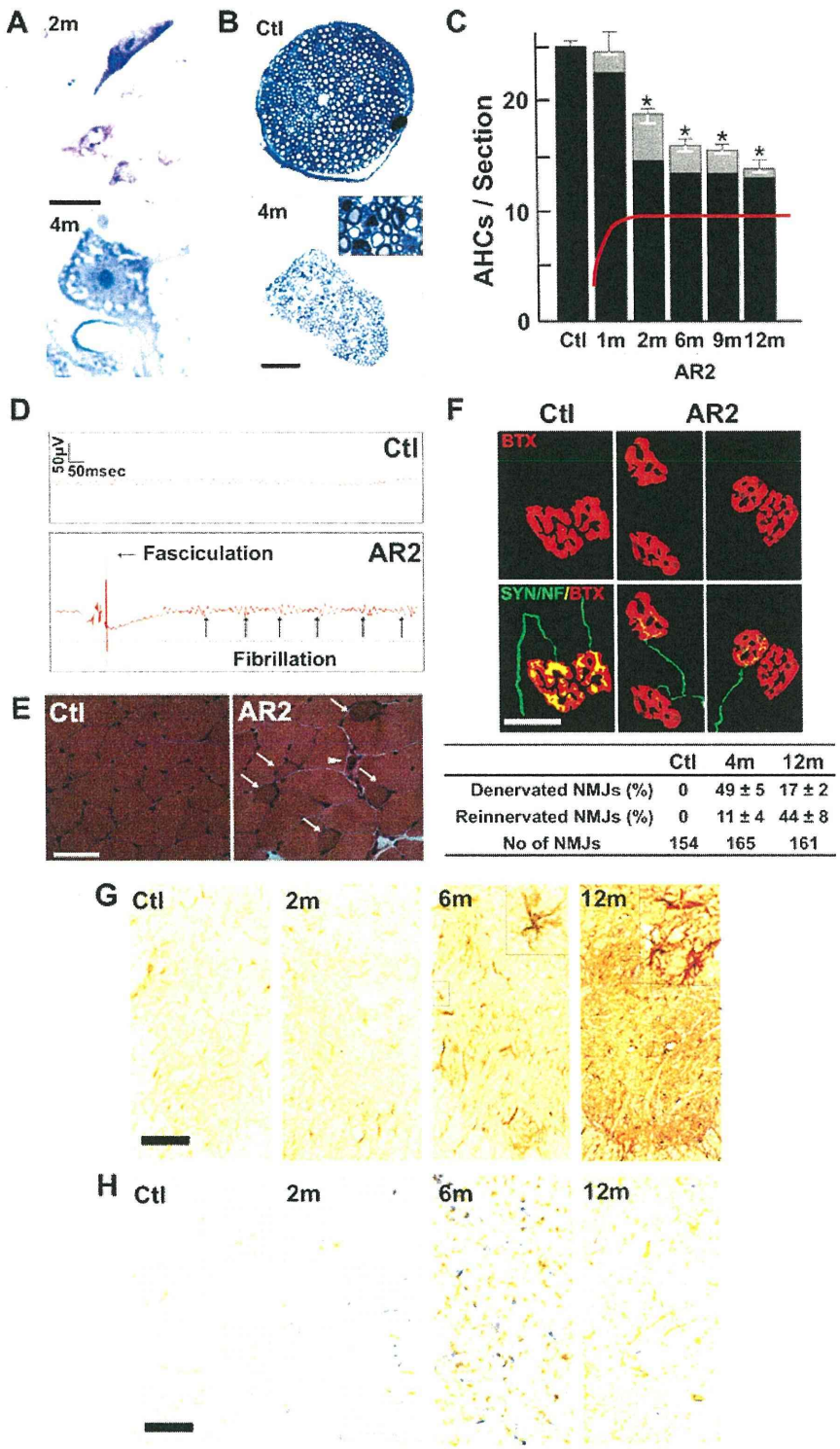

	Ctl	4m	12m
Denervated NMJs (%)	0	49 ± 5	17 ± 2
Reinnervated NMJs (%)	0	11 ± 4	44 ± 8
No of NMJs	154	165	161

Figure 4. Loss of ADAR2-deficient motor neurons. ***A***, Degenerating AHCs in AR2 mice at 2 months (2m; Nissl staining) and 4 months (4m; toluidine blue staining, 1 μm section) of age. Scale bar: 2m, 25 μm; 4m, 12.5 μm. ***B***, Ventral root (L5) of control (Ctl) and AR2 mice at 4 months of age (4m). Inset, Magnified view of degenerating axons. Scale bar: 100 μm; inset, 20 μm. ***C***, Numbers of AHCs showing ADAR2 immunoreactivity (black columns) and lacking this immunoreactivity (gray columns) (mean ± SEM) in AR2 mice at different ages (1m, 2m, 6m, 9m, 12m). In AR2 mice, Cre expression is developmentally regulated (orange line), and ~50% of motor neurons express Cre by 5 weeks of age, with recombination of the *ADAR2* gene in ~10% of AHCs at 1 month of age and 40–45% of AHCs after 2 months of age (orange line). The number of ADAR2-lacking AHCs significantly decreased in AR2 mice after 2 months of age as a result of Cre-dependent knock-out of ADAR2 (*$p < 0.01$, repeated-measures ANOVA). The number of AHCs in the control mice did not change at different ages, and all the AHCs in controls showed ADAR2 immunoreactivity. ***D***, Electrophysiological examination in AR2 mice. Electromyography from an AR2 mouse at 12 months of age showing fibrillations and fasciculations, common findings in ALS indicative of muscle fiber denervation and motor unit degeneration and regeneration. These findings were observed in two other AR2 mice examined but never in control mice (Ctl; $n = 2$). ***E***, Calf muscles from a wild-type mouse (left) and an AR2 mouse (middle and right) at 12 months of age. Characteristics of denervated muscles, including muscle fiber atrophy (white arrow), centrally placed nuclei, and pyknotic nuclear clumps (white arrowhead) are observed in the AR2 mouse. Hematoxylin and eosin. Scale bar, 60 μm. ***F***, NMJs and distal axons. Quadriceps muscles from a wild-type mouse (Ctl; left) and an AR2 mouse (AR2; middle and right) at 12 months of age are stained with tetramethylrhodamine–bungarotoxin (BTX) (red) and immunostained concomitantly with anti-synaptophysin and neurofilament (SYN/NF) antibodies (green). Endplates (red) were counted as "innervated" if they were merged with axon terminals (merge; yellow). Each endplate is innervated by a thick axon terminal in the Ctl mouse. In AR2 mice, in addition to the normally innervated NMJs, some NMJs were innervated by axons that simultaneously innervate more than one NMJ (reinnervated NMJs; middle), and other NMJs were devoid of axon terminals (denervated NMJs; right). More than 50 NMJs were counted in each animal in the control group and groups of AR2 mice at 4 and 12 months of age ($n = 3$ in each group). Proportions of denervated NMJs and reinnervated NMJs among total NMJs in each group are indicated as mean ± SD (percentage). Scale bar, 25 μm. ***G***, ***H***, Immunohistochemistry in the anterior horn (C5). There was a time-dependent increase in GFAP immunoreactivity (***G***) and an increase in MAC2 immunoreactivity maximal at 6 months of age (***H***) in the spinal anterior horn of AR2 mice. m, Months of age; inset, activated astroglia. Scale bars: ***G***, 100 μm; insets and ***H***, 50 μm.

editing, mean ± SEM: for AR2 mice, 89.7 ± 5.8%, $n = 3$; for control mice, 100%, $n = 3$, $p = 0.0048$) and in the facial nerve nuclei (for AR2 mice, 82.6 ± 9.1%, $n = 3$; for control mice, 99.2 ± 0.2%, $n = 3$, $p = 0.0017$) of AR2 mice at 12 months of age. These results indicate that ADAR2-lacking motor neurons do not always undergo cell death, and some motor neurons, including those in the oculomotor nerve nucleus, are relatively resistant to cell death mediated by deficient ADAR2. Indeed, motor neurons innervating extraocular muscles are much less vulnerable than those innervating bulbar and limb muscles in ALS patients (Lowe and Leigh, 2002).

GluR-B^R alleles prevent motor neuron death in AR2 mice

To investigate by genetic means the role of RNA editing at the GluR2 Q/R site in the death of motor neurons, we exchanged the endogenous *GluR2* alleles in AR2 mice with GluR-B^R alleles (Kask et al., 1998), which directly encode Q/R site-edited GluR2, thus circumventing the requirement for ADAR2-mediated RNA editing. AR2/GluR-$B^{R/R}$ mice were obtained by $ADAR2^{flox/+}$/VAChT–Cre.Fast/GluR-$B^{R/+}$ mice intercrosses to generate $ADAR2^{flox/flox}$/VAChT–Cre.Fast/GluR-$B^{R/R}$ (AR2/GluR-$B^{R/R}$) mice (see Materials and Methods).

Table 1. Density of neurons in motor nerve nuclei and spinal cord

Nucleus	Control ($n = 3$) neurons/mm^3	AR2 ($n = 4$) neurons/mm^3
III	11,253 ± 1783	10,441 ± 632
IV	15,783 ± 1694	16,032 ± 658
VI	10,117 ± 996	10,699 ± 195
Vm	8809 ± 417	8623 ± 246
Vm (>25 μm)	3603 ± 213	2767 ± 175**
VII	1041 ± 124	1016 ± 96
VII (>20 μm)	91.1 ± 32.7	67.7 ± 13.1**
X	11,442 ± 1932	11,652 ± 2387
XII	11,800 ± 541	9834 ± 1530
XII (>20 μm)	832.7 ± 92.9	677.8 ± 116.2**
C5 AH (≤20 μm)	37,147 ± 326	37,941 ± 331
C5 AH (>20 μm)	25.5 ± 0.9[a]	13.7 ± 0.7[a,**]
L5 AH (>20 μm)	29.3 ± 0.32[a]	15.9 ± 0.31[a,**]
DH	476,312 ± 12,623	498,816 ± 21,446
VR	840.0 ± 26.5[b]	626.3 ± 31.4[b,*]

Numbers are the neuronal density per cubic millimeter (mean ± SEM) in each nucleus from mice at 12 months of age. For Vm, VII, and XII, neurons with large diameter (>20 or 25 μm) were also counted. AR2, *ADAR2*$^{flox/flox}$/VAChT–Cre.Fast mice; III, nucleus of oculomotor nerve; IV, nucleus of trochlear nerve; VI, nucleus of abducens nerve; Vm, motor nucleus of trigeminal nerve; VII, nucleus of facial nerve; X, dorsal nucleus of the vagus nerve; XII, nucleus of hypoglossal nerve; C5 AH, anterior horn of the fifth cervical cord; L5 AH, anterior horn of the fifth lumbar cord; DH, zona gelatinosa of the spinal cord; VR, ventral roots (L5). *$p < 0.005$; **$p < 0.001$ (ANOVA).

[a]Number of neurons per section.

[b]Number of axons.

AR2/GluR-$B^{R/R}$ mice (AR2rescue, or AR2res, mice) were phenotypically normal and had full motor function until 6 months of age (Fig. 5*A*). The AHCs, including the ~30% AHCs lacking ADAR2 from Cre-mediated recombination, were viable in AR2res mice at 6 months of age, and the total number of AHCs was the same as in age-matched control mice (Fig. 5*A*,*B*). Consistent with a lack of AHC loss, there was no detectable increase in GFAP or MAC2 immunoreactivity in the anterior horns (supplemental Fig. S2*C*, available at www.jneurosci.org as supplemental material). These results demonstrate that it is specifically the failure of GluR2 Q/R site editing by which ADAR2 deficiency induces the slow death of motor neurons (Fig. 5*C*).

Discussion

We generated the AR2 mouse (Hideyama et al, 2008), a conditional ADAR2 knock-out line, which carries gene-targeted floxed ADAR2 alleles that become functionally ablated by Cre recombinase expressed from a transgene (VAChT–Cre.Fast) in ~50% of motor neurons (Misawa et al., 2003). These displayed progressive motor dysfunctions. The ADAR2-lacking motor neurons expressed only Q/R site-unedited GluR2. Virtually all of the ADAR2-lacking AHCs underwent degeneration, whereas the surviving ADAR2-expressing AHCs remained intact by 12 months of age. The death of ADAR2-lacking AHCs was completely prevented by a point mutation in the endogenous GluR2 alleles of AR2 mice, thus generating Q/R site-edited GluR2 in the absence of ADAR2 (Kask et al., 1998). These findings highlight the crucial role of RNA editing at the GluR2 Q/R site for survival of motor neurons and demonstrate that expression of Q/R site-unedited GluR2 is a cause of slow death of motor neurons. Therefore, it is necessary to investigate the relevance of inefficient GluR2 Q/R site-RNA editing found in the patient's motor neurons to the pathogenesis of sporadic ALS (Kawahara et al., 2004; Kwak and Kawahara, 2005).

Concomitant with the loss of ADAR2-lacking AHCs, proximal and distal axons of AHCs underwent degeneration with resultant neurogenic changes in neuromuscular units. These pathological changes in AHCs and neuromuscular units caused motor dysfunctions in AR2 mice. The prevention of slow neuronal cell death observed in AR2 mice by GluR-B^R alleles expressing Q/R site-edited GluR2 in the absence of ADAR2 (Kask et al., 1998) means that, although ADAR2 edits numerous A-to-I positions in many RNAs expressed in the mammalian brain (Levanon et al., 2004; Li et al., 2009), failure of A-to-I conversions at sites other than the GluR2 Q/R site did not play a role in neuronal cell death (Fig. 5*C*).

When the GluR2 Q/R site is unedited, the Ca^{2+} permeability of the AMPA receptor is greatly increased, and trafficking of the receptor to synaptic membranes is facilitated (Sommer et al., 1991; Burna-

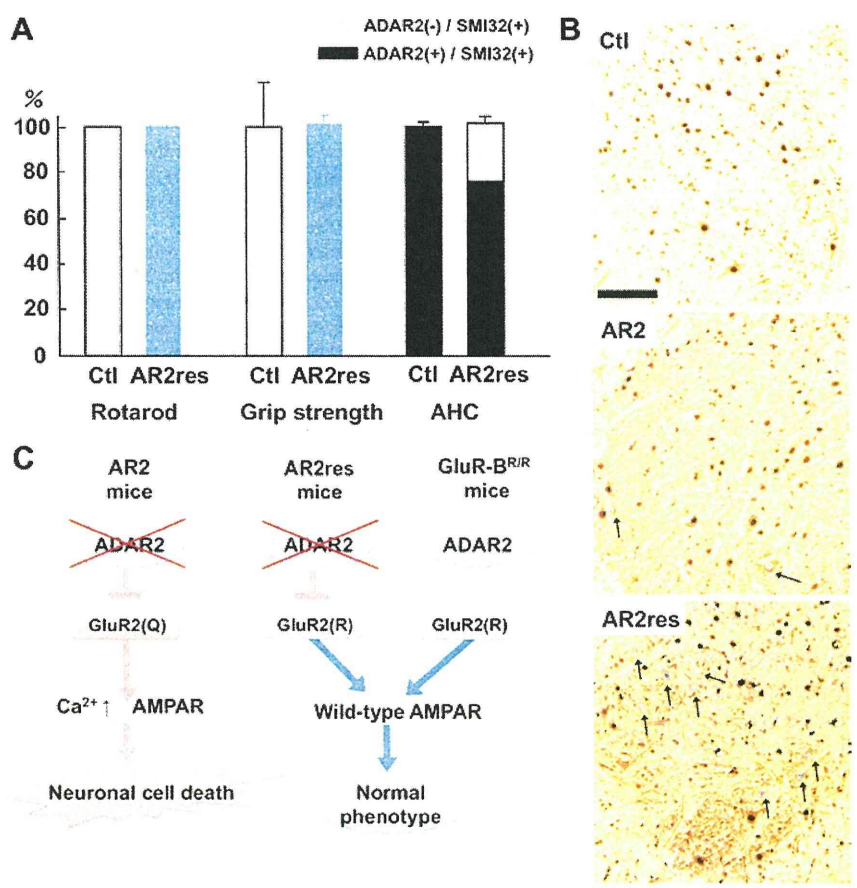

Figure 5. Crucial role of GluR2 Q/R site editing in death of ADAR2-deficient motor neurons. ***A***, AR2/GluR-$B^{R/R}$ mice (AR2res) displayed full rotarod score and normal grip strength at 6 months of age compared with control mice (Ctl). The number of total AHCs, of which a considerable proportion was deficient in ADAR2, did not decrease in AR2res mice. ***B***, At 6 months of age, although only a few AHCs lacking ADAR2 immunoreactivity (arrowheads) were observed in AR2 mice, a considerable number of AHCs lacking ADAR2 immunoreactivity was present in AR2res mice. The density of AHCs in AR2res mice was similar to that in the control mice in which all the AHCs were immunoreactive to ADAR2 in their nuclei. Sections were counterstained with hematoxylin. Scale bar, 100 μm. ***C***, Scheme illustrating that lack of ADAR2 induces slow death of motor neurons in AR2 mice but not in AR2res mice that express Q/R site-edited GluR2 in the absence of ADAR2 activity. The exonic Q codon at the Q/R site of GluR2 was substituted by an R codon in the endogenous GluR2 alleles of GluR-$B^{R/R}$ mice.

shev et al., 1992; Greger et al., 2002). This enhances neuronal excitability by increasing the density of Ca^{2+}-permeable functional AMPA channels, which is typically observed as fatal epilepsy in mice carrying Q/R site-uneditable GluR-*B* (*GluR2*) alleles (Brusa et al., 1995; Feldmeyer et al., 1999) and in systemic ADAR2-null mice (Higuchi et al., 2000). The results obtained from AR2 mice indicate that motor neurons expressing only Q/R site-unedited GluR2 undergo slow death when the mice live sufficiently long.

Some ADAR2-lacking AHCs die shortly after recombination, whereas others survive for more than 1 year. These observations indicate that, although all the ADAR2-lacking AHCs undergo neuronal death, the ability to compensate for the increased Ca^{2+} overload through the functionally altered AMPA receptor differs among AHCs. It is likely that the increased Ca^{2+} overload might have already led to dysfunction of the ADAR2-lacking AHCs before their death, causing a decline of motor functions at earlier stages. Vulnerability of motor neurons to Ca^{2+}-permeable AMPA receptor-mediated toxicity was demonstrated in GluR-B(N) transgenic mice, which additionally to wild-type GluR2 express an engineered GluR2 subunit that features asparagine (N) in place of glutamine (Q) at the Q/R site (Kuner et al., 2005). ADAR2 activity is downregulated in the rat after transient forebrain ischemia, resulting in the selective death of hippocampal CA1 pyramidal cells (Peng et al., 2006).

An intriguing observation in AR2 mice was the selective vulnerability among motor neurons in different cranial nerve nuclei. Neurons in facial and hypoglossal nerve nuclei decreased in number, whereas those in the oculomotor nerve nuclei did not, although the extent of GluR2 Q/R site editing was significantly reduced in all these nuclei. These results indicate that motor neurons in the oculomotor nerve nuclei can survive despite the incomplete nature of GluR2 Q/R site editing. Notably, motor neurons in the nuclei of oculomotor nerves are also much less vulnerable in ALS patients; this has been attributed to differential expression levels of Ca^{2+}-binding proteins, particularly parvalbumin, among motor neurons in different cranial nerve nuclei. Expression of parvalbumin is high in oculomotor neurons and low in the facial and spinal motor neurons (Ince et al., 1993). Indeed, overexpression of parvalbumin attenuated kainate-induced Ca^{2+} transients and protected spinal motor neurons from resultant neurotoxicity in parvalbumin transgenic mice (Van Den Bosch et al., 2002). It is likely that neurons with an efficient Ca^{2+}-buffering system, such as oculomotor neurons, are resistant to Ca^{2+} overload resulting from Ca^{2+}-permeable AMPA receptors.

The present results indicate that the failure of A-to-I conversion at the Q/R site of GluR2 pre-mRNA in motor neurons of sporadic ALS patients (Takuma et al., 1999; Kawahara et al., 2004; Kwak and Kawahara, 2005) is likely attributable to reduced ADAR2 activity. Indeed, the expression level of ADAR2 mRNA was decreased in the spinal cord of patients with sporadic ALS (Kawahara and Kwak, 2005). Molecular abnormalities found in postmortem tissues of patients with neurodegenerative diseases have shown signs of mechanisms underlying the disease and may represent both the neuronal death process and death-protective reactions arising from the protracted nature of the death process. It is therefore necessary to determine whether these molecular abnormalities are the cause or the result of neuronal cell death by developing an appropriate animal model. Although excitotoxicity has long been implicated in the pathogenesis of neurological diseases including ALS (Vosler et al., 2008; Bezprozvanny, 2009), surprisingly little direct evidence indicating excitotoxic neuronal cell death has been demonstrated in patient-derived materials. Here we demonstrate that the molecular abnormality found in motor neurons of patients with sporadic ALS is a direct cause of neuronal death in mice via a mechanism upregulating Ca^{2+}-permeable AMPA receptors. In addition, the AR2 mice possess certain characteristics found in ALS, including slow progressive death of motor neurons, neuromuscular unit-dependent motor dysfunction and differential low vulnerability of motor neurons of extraocular muscles. Therefore, this mouse model mimicking patient-derived molecular abnormalities may be useful for research on sporadic ALS.

References

Akbarian S, Smith MA, Jones EG (1995) Editing for an AMPA receptor subunit RNA in prefrontal cortex and striatum in Alzheimer's disease, Huntington's disease and schizophrenia. Brain Res 699:297–304.

Beleza-Meireles A, Al-Chalabi A (2009) Genetic studies of amyotrophic lateral sclerosis: controversies and perspectives. Amyotroph Lateral Scler 10:1–14.

Bezprozvanny I (2009) Calcium signaling and neurodegenerative diseases. Trends Mol Med 15:89–100.

Brusa R, Zimmermann F, Koh DS, Feldmeyer D, Gass P, Seeburg PH, Sprengel R (1995) Early-onset epilepsy and postnatal lethality associated with an editing-deficient GluR-B allele in mice. Science 270:1677–1680.

Burnashev N, Monyer H, Seeburg PH, Sakmann B (1992) Divalent ion permeability of AMPA receptor channels is dominated by the edited form of a single subunit. Neuron 8:189–198.

Carriedo SG, Yin HZ, Weiss JH (1996) Motor neurons are selectively vulnerable to AMPA/kainate receptor-mediated injury *in vitro*. J Neurosci 16:4069–4079.

Feldmeyer D, Kask K, Brusa R, Kornau HC, Kolhekar R, Rozov A, Burnashev N, Jensen V, Hvalby O, Sprengel R, Seeburg PH (1999) Neurological dysfunctions in mice expressing different levels of the Q/R site-unedited AMPAR subunit GluR-B. Nat Neurosci 2:57–64.

Feng Y, Sansam CL, Singh M, Emeson RB (2006) Altered RNA editing in mice lacking ADAR2 autoregulation. Mol Cell Biol 26:480–488.

Greger IH, Khatri L, Ziff EB (2002) RNA editing at arg607 controls AMPA receptor exit from the endoplasmic reticulum. Neuron 34:759–772.

Greger IH, Khatri L, Kong X, Ziff EB (2003) AMPA receptor tetramerization is mediated by Q/R editing. Neuron 40:763–774.

Hideyama T, Yamashita T, Tsuji S, Misawa H, Takahashi R, Suzuki T, Kwak S (2008) Slow neuronal death of motor neurons in sporadic ALS mouse model by RNA editing enzyme ADAR2 knockout. Soc Abstr Neurosci 34:745.17.

Higuchi M, Maas S, Single FN, Hartner J, Rozov A, Burnashev N, Feldmeyer D, Sprengel R, Seeburg PH (2000) Point mutation in an AMPA receptor gene rescues lethality in mice deficient in the RNA-editing enzyme ADAR2. Nature 406:78–81.

Ince P, Stout N, Shaw P, Slade J, Hunziker W, Heizmann CW, Baimbridge KG (1993) Parvalbumin and calbindin D-28k in the human motor system and in motor neuron disease. Neuropathol Appl Neurobiol 19:291–299.

Kask K, Zamanillo D, Rozov A, Burnashev N, Sprengel R, Seeburg PH (1998) The AMPA receptor subunit GluR-B in its Q/R site-unedited form is not essential for brain development and function. Proc Natl Acad Sci U S A 95:13777–13782.

Kawahara Y, Kwak S (2005) Excitotoxicity and ALS: what is unique about the AMPA receptors expressed on spinal motor neurons? Amyotroph Lateral Scler Other Motor Neuron Disord 6:131–144.

Kawahara Y, Ito K, Sun H, Kanazawa I, Kwak S (2003a) Low editing efficiency of GluR2 mRNA is associated with a low relative abundance of ADAR2 mRNA in white matter of normal human brain. Eur J Neurosci 18:23–33.

Kawahara Y, Kwak S, Sun H, Ito K, Hashida H, Aizawa H, Jeong SY, Kanazawa I (2003b) Human spinal motoneurons express low relative abundance of GluR2 mRNA: an implication for excitotoxicity in ALS. J Neurochem 85:680–689.

Kawahara Y, Ito K, Sun H, Aizawa H, Kanazawa I, Kwak S (2004) Glutamate receptors: RNA editing and death of motor neurons. Nature 427:801.

Kawahara Y, Sun H, Ito K, Hideyama T, Aoki M, Sobue G, Tsuji S, Kwak S (2006) Underediting of GluR2 mRNA, a neuronal death inducing mo-

lecular change in sporadic ALS, does not occur in motor neurons in ALS1 or SBMA. Neurosci Res 54:11–14.

Kuner R, Groom AJ, Bresink I, Kornau HC, Stefovska V, Müller G, Hartmann B, Tschauner K, Waibel S, Ludolph AC, Ikonomidou C, Seeburg PH, Turski L (2005) Late-onset motoneuron disease caused by a functionally modified AMPA receptor subunit. Proc Natl Acad Sci U S A 102: 5826–5831.

Kwak S, Kawahara Y (2005) Deficient RNA editing of GluR2 and neuronal death in amyotropic lateral sclerosis. J Mol Med 83:110–120.

Levanon EY, Eisenberg E, Yelin R, Nemzer S, Hallegger M, Shemesh R, Fligelman ZY, Shoshan A, Pollock SR, Sztybel D, Olshansky M, Rechavi G, Jantsch MF (2004) Systematic identification of abundant A-to-I editing sites in the human transcriptome. Nat Biotechnol 22:1001–1005.

Li JB, Levanon EY, Yoon JK, Aach J, Xie B, Leproust E, Zhang K, Gao Y, Church GM (2009) Genome-wide identification of human RNA editing sites by parallel DNA capturing and sequencing. Science 324:1210–1213.

Lowe JS, Leigh N (2002) Motor neuron disease (amyotrophic lateral sclerosis). In: The Greenfield's neuropathology (Love S, Louis DN, Ellison DW, eds), pp 372–383. Oxford: Oxford UP.

Melcher T, Maas S, Herb A, Sprengel R, Seeburg PH, Higuchi M (1996) A mammalian RNA editing enzyme. Nature 379:460–464.

Misawa H, Nakata K, Toda K, Matsuura J, Oda Y, Inoue H, Tateno M, Takahashi R (2003) VAChT–Cre.Fast and VAChT–Cre.Slow: postnatal expression of Cre recombinase in somatomotor neurons with different onset. Genesis 37:44–50.

Nishimoto Y, Yamashita T, Hideyama T, Tsuji S, Suzuki N, Kwak S (2008) Determination of editors at the novel A-to-I editing positions. Neurosci Res 61:201–206.

Ohmae S, Takemoto-Kimura S, Okamura M, Adachi-Morishima A, Nonaka M, Fuse T, Kida S, Tanji M, Furuyashiki T, Arakawa Y, Narumiya S, Okuno H, Bito H (2006) Molecular identification and characterization of a family of kinases with homology to Ca^{2+}/calmodulin-dependent protein kinases I/IV. J Biol Chem 281:20427–20439.

Paschen W, Hedreen JC, Ross CA (1994) RNA editing of the glutamate receptor subunits GluR2 and GluR6 in human brain tissue. J Neurochem 63:1596–1602.

Paxinos G, Franklin KBJ (2001) The mouse brain in stereotaxic coordinates. San Diego: Academic.

Peng PL, Zhong X, Tu W, Soundarapandian MM, Molner P, Zhu D, Lau L, Liu S, Liu F, Lu Y (2006) ADAR2-dependent RNA editing of AMPA receptor subunit GluR2 determines vulnerability of neurons in forebrain ischemia. Neuron 49:719–733.

Rothstein JD, Martin LJ, Kuncl RW (1992) Decreased glutamate transporter by the brain and spinal cord in amyotrophic lateral sclerosis. N Engl J Med 326:1464–1468.

Sansam CL, Wells KS, Emeson RB (2003) Modulation of RNA editing by functional nucleolar sequestration of ADAR2. Proc Natl Acad Sci U S A 100:14018–14023.

Schymick JC, Talbot K, Traynor BJ (2007) Genetics of sporadic amyotrophic lateral sclerosis. Hum Mol Genet 16 [Spec No 2]:R233–R242.

Seeburg PH (2002) A-to-I editing: new and old sites, functions and speculations. Neuron 35:17–20.

Sommer B, Köhler M, Sprengel R, Seeburg PH (1991) RNA editing in brain controls a determinant of ion flow in glutamate-gated channels. Cell 67:11–19.

Suzuki T, Tsuzuki K, Kameyama K, Kwak S (2003) Recent advances in the study of AMPA receptors. Nippon Yakurigaku Zasshi 122:515–526.

Takemoto-Kimura S, Ageta-Ishihara N, Nonaka M, Adachi-Morishima A, Mano T, Okamura M, Fujii H, Fuse T, Hoshino M, Suzuki S, Kojima M, Mishina M, Okuno H, Bito H (2007) Regulation of dendritogenesis via a lipid-raft-associated Ca^{2+}/calmodulin-dependent protein kinase CLICK-III/CaMKIgamma. Neuron 54:755–770.

Takuma H, Kwak S, Yoshizawa T, Kanazawa I (1999) Reduction of GluR2 RNA editing, a molecular change that increases calcium influx through AMPA receptors, selective in the spinal ventral gray of patients with amyotrophic lateral sclerosis. Ann Neurol 46:806–815.

Van Damme P, Bracken D, Callewaert G, Robberecht W, Van Den Bosch L (2005) GluR2 deficiency accelerates motor neuron degeneration in a mouse model of amyotrophic lateral sclerosis. J Neuropathol Exp Neurol 64:605–612.

Van Den Bosch L, Schwaller B, Vleminckx V, Meijers B, Stork S, Ruehlicke T, Van Houtte E, Klaassen H, Celio MR, Missiaen L, Robberecht W, Berchtold MW (2002) Protective effect of parvalbumin on excitotoxic motor neuron death. Exp Neurol 174:150–161.

Vosler PS, Brennan CS, Chen J (2008) Calpain-mediated signaling mechanisms in neuronal injury and neurodegeneration. Mol Neurobiol 38: 78–100.

Yang JH, Sklar P, Axel R, Maniatis T (1995) Editing of glutamate receptor subunit B pre-mRNA in vitro by site-specific deamination of adenosine. Nature 374:77–81.

Table S1. Sequence of materials used

pLF Neo-PLUS selection cassette in ADAR2^{flox}
5'---GGCCATAGCGGCCGGCC**ATAACTTCGTATAGCATACATTAT**GGCGCGGAGTCGACGAT C*AAGCTT*TCGAAGATCTACGT*GGCGCGCC*CTCGAGCTTTCG***GAAGTTCCTATTCGGAAGTTC*** ***CTATTCTCTAGAAAGTATAGGAACTTC***TCGAGATCCGATATCGAATTCCCGCGCCCCCAGCTG GTTCTTTCCGCCTCAGAAGCCATAGAGCCCACCGCATCCCCAGCATGCCTGCTATTGTCTTC CCAATCCTCCCCCTTGCTGTCCTGCCCCACCCCACCCCCCAGAATAGAATGACACCTACTCA GACAATGCGATGCAATTTCCTCATTTTATTAGGAAAGGACAGTGGGAGTGGCACCTTCCAG GGTCAAGGAAGGCACGGGGGAGGGGCAAACAACAGATGGCTGGCAACTAGAAGGCACAG TCGAGGCTGATCAGCGAGCTCTAGAGAATTGATCCCCTCAGAAGAACTCGTCAAGAAGGCG ATAGAAGGCGATGCGCTGCGAATCGGGAGCGGCGATACCGTAAAGCACGAGGAAGCGGTC AGCCCATTCGCCGCCAAGCTCTTCAGCAATATCACGGGTAGCCAACGCTATGTCCTGATAGC GATCCGCCACACCCAGCCGGCCACAGTCGATGAATCCAGAAAAGCGGCCATTTTCCACCAT GATATTCGGCAAGCAGGCATCGCCATGGGTCACGACGAGATCCTCGCCGTCGGGCATGCGC GCCTTGAGCCTGGCGAACAGTTCGGCTGGCGCGAGCCCCTGATGCTCTTCGTCCAGATCAT CCTGATCGACAAGACCGGCTTCCATCCGAGTACGTGCTCGCTCGATGCGATGTTTCGCTTGG TGGTCGAATGGGCAGGTAGCCGGATCAAGCGTATGCAGCCGCCGCATTGCATCAGCCATGA TGGATACTTTCTCGGCAGGAGCAAGGTGAGATGACAGGAGATCCTGCCCCGGCACTTCGCC CAATAGCAGCCAGTCCCTTCCCGCTTCAGTGACAACGTCGAGCACAGCTGCGCAAGGAAC GCCCGTCGTGGCCAGCCACGATAGCCGCGCTGCCTCGTCCTGCAGTTCATTCAGGGCACCG GACAGGTCGGTCTTGACAAAAAGAACCGGGCGCCCCTGCGCTGACAGCCGGAACACGGCG GCATCAGAGCAGCCGATTGTCTGTTGTGCCCAGTCATAGCCGAATAGCCTCTCCCAAGGCG GCCGGAGAACCTGCGTGCAATCCATCTTGTTCAATGGCCGATCCCATTATGACCTGCAGGTC GAAAGGCCCGGAGATGAGGAAGAGGAGAACAGCGCGGCAGACGTGCGCTTTTGAAGCGT GCAGAATGCCGGGCCCTCCGGAGGACCTTCGCGCCCGCCCCGCCCCTGAGCCCGCCCCTGA GCCCGCCCCCGGACCCACCCCTTCCCAGCCTCTGAGCCCAGAAAGCGAAGGAGCCAAGCT GCTATTGGCCGCTGCCCCAAAGGCCTACCCGCTTCCATTGCTCAGCGGTGCTGTCCATCTGC ACGAGACTAGTGAGACGTGCTACTTCCATTTGTCACGTCCTGCACGACGCGAGCTGCGGGG CGGGGGGGAACTTCCTGACTAGGGGAGGAGTAGAAGGTGGCGCGAAGGGGCCACCAAAG AACGGAGCCGGTTGGCGCCTACCGGTGGATGTGGAATGTGTGCGAGGCCAGAGGCCACTT GTGTAGCGCCAAGTGCCCAGCGGGGCTGCTAAAGCGCATGCTCCAGACTGCCTTGGGAAA AGCGCCTCCCCTACCCGGTAGGGCGCGGGAATTCGATATCGAATTCGAGCTCGGTACCCGG GGATCGAAGTTCCTATTCG***GAAGTTCCTATTCTCTAGAAAGTATAGGAACTTC***TCGACCTGCA GGCATGCAAGCTGATCCGGCGCGT**ATAACTTCGTATAGCATACATTATACGAAGTTAT**CCT CAGGCCAGCGAGGCC---3' (SfiI sites that flank the cassette are underlined. The 5' and 3' **Lox P sites** are in **bold**. The 5' and 3' ***FRT sites*** are in ***bold italics***. The floxed region (2623bp, exons 7-9: nt 14,452-17,075 from the contig above) was subcloned into the HindIII/AscI sites (italics, underlined).)

Primers used for PCR and RT-PCR

GluR2 (Accession no. NM_001039195, NM_001083806) Q/R site
5'-AGCAGATTTAGCCCCTACGAG-3'/5'-CAGCACTTTCGATGGGAGACAC-3
(Amplified product length: 278; *BbvI*; Ed: 219, 59; Uned: 140, 79, 59; Eff: 219/59)
Pre-mRNA GluR2 (Accession no. NM_001039195, NM_001083806) Q/R site
5'-CAGCAGATTTAGCCCCTACGA-3'/5'-CAGGAACATTGTTCAGGTAATTCACAG-3'
(Amplified product length: 335; *BbvI*; Ed: 242, 93; Uned: 126, 116, 93; Eff: 242/93)
GluR2 (Accession no. NM_001039195, NM_001083806) R/G site
5'-AGGAAATCCAAAGGGAAGT-3'/5'-CTGTGTTTGTGAGGACTAC-3'
(Amplified product length: 256; *BbvI*; Ed: 214, 9, 33; Uned: 144, 70, 9, 33; Eff: 214/33)
GluR5 (Accession no. NM_008168, NM_000828, NM_146072)
5'-TAGTTTCTGGTTTGGCGTTG-3'/ 5'-GACTGCCCCGTATTCTATCT-3'
(Amplified product length: 226; *BbvI*; Ed: 32, 194; Uned: 32, 104, 90; Eff: 194/32)
GluR6 (Accession no. NM_010349, X66117.1)
1st PCR 5'-TTCCTGAATCCTCTCTCCCT-3'/5'-CACCAAATGCCTCCCACTATC-3'
(Amplified product length: 260)
Nested PCR 5'-TTTGTCATAGCCAGGTTTAGTCC-3'/5'-CCAAATGCCTCCCACTATCC-3'
(Amplified product length: 186; *BbvI*; Ed: 186; Uned: 136, 50; Eff: 186 /(186 + 136))
Kv1.1 (Accession no. NM_010595)
5'-TTGGACACAATGACAGGTA-3'/5'-TGTTTTCTAGCGCAGTGT-3'
(Amplified product length: 213; *MfeI*; Ed: 130,83; Uned: 130, 51, 32; Eff: 81 /130)
VAChT-Cre (Misawa et al., 2003)
5'-ACCTGATGGACATGTTCAGG-3'/5'-CGAGTTGATAGCTGGCTGG-3'
(Amplified product length: 701)
ADAR2^{flox} (Accession no. NM_001024840, AF403109, see below)
(F1/R1) 5'-CTGGTTCATAACAGATCCTCAGGG-3' /5'-GTCTCCCTTGTCCTTCCAGGTAGC-3'
(Amplified product length: 2817)
ADAR2 (Accession no. NM_001024840, AF403109)
(F2/R2) 5'-AAGAAGGAATCCAGCGAGTCC-3' /5'-ATTGCCCCTCCACCATTTC-3'
(Amplified product length: 692)
GluR-B^{R} (Kask et al., 1998)
5'-GTTGATCATGTGTTTCCCTG-3'/5'-CAATAGCAATTGGTGATTTGTGAC-3'
(Amplified product length: wild-type: 494; GluR-B^{R}: 599)
β-actin (Accession no. X03672)
1st PCR 5'-AGCTTCTTTGCAGCTCCTTCGTT-3' /5'-GAGCCACCGATCCACACAGAG-3'
(Nihon Gene Research Lab's Inc., Sendai, Japan) (Amplified product length: 1082)
Nested PCR 5'-CGTTGACATCCGTAAAGACCTC-3' /5'-AGCCACCGATCCACACAGA-3'
(Nihon Gene Research Lab's Inc., Sendai, Japan)(Amplified product length: 155)
ChAT (Accession no. NM_009891) (Zhang et al., 2007)
1st PCR 5'-TCCTGGACATGATCGAG-3' /5'-ACGATGCCATCAAAAGGG-3'
(Amplified product length: 218)
Nested PCR 5'-CCTGGATGGTCCAGGCACT-3'/5'-GTCATACCAACGATTCGCTCC-3'
(Amplified product length: 102)

Enz, restriction enzyme; Ed, length (bp) of restriction digests of PCR products from edited mRNA; Uned, length (bp) of restriction digests of PCR products from united mRNA; Eff, bands used for the calculation of the editing efficiency.

Target sequence of ADAR2 mRNA for *in situ* hybridization (Fig. 1c)
5'-AGGTACAGATGTCAAAGATGCCAAGGTGATAAGTGTTTCGACAGGGACGAAGTGTATCAACG GTGAATACATGAGTGACCGTGGCCTCGCACTCAATGACTGCCACGCAGAGATAATCTCCCGAAG GTCCCTGCTCAGGTTTCTTTATGCACAGCTCGAGCTTTATTTAAATAACAAAGAAGACCAGAAA AAGTCCATATTTCAGAAGTCAGAGCGGGGTGGGTTCCGGCTGAAGGATACCGTGCAGTTCCACC TGTACATCAGCACCTCGCCCTGCGGAGACGCCAGAATATTCTCTCCCCACGAGCCCGTGCTAGA GGGTATGACGCCAGACTCTCACCAGCTGACAGAACCAGCAGATAGACATCCGAATCGCAAAGC AAGGGGACAG-3'

Supplementary reference

Kask K, Zamanillo D, Rozov A, Burnashev N, Sprengel R, Seeburg PH (1998) The AMPA receptor subunit GluR-B in its Q/R site-unedited form is not essential for brain development and function. Proc Natl Acad Sci U S A 95:13777-13782.

Misawa H, Nakata K, Toda K, Matsuura J, Oda Y, Inoue H, Tateno M, Takahashi R (2003) VAChT-Cre.Fast and VAChT-Cre.Slow: postnatal expression of Cre recombinase in somatomotor neurons with different onset. Genesis 37:44-50.

Zhang Y, Cardell LO, Adner M (2007) IL-1beta induces murine airway 5-HT2A receptor hyperresponsiveness via a non-transcriptional MAPK-dependent mechanism. Respir Res. 8: 29-40

Table S2. Predicted number of ADAR2-null motor neurons in each ADAR2$^{flox/flox}$/VAChT-Cre.Fast (AR2) mouse

Group	0:3			1:2			2:1			3:0			Total		
AR2 mouse	Number of specimens	Number of neurons		Number of specimens	Number of neurons		Number of specimens	Number of neurons		Number of specimens	Number of neurons		Number of specimens	Number of neurons	
		Ed	Uned		Ed	Uned		Ed	Uned		Ed	Uned		Ed	Uned (%)
#1	3	0	9	4	4	8	1	2	1	12	36	0	20	42	18 (30.0)
#2	2	0	6	4	4	8	18	36	18	7	21	0	31	61	32 (34.4)
#3	2	0	6	6	6	12	13	26	13	14	42	0	35	74	31 (29.5)
#4	1	0	3	6	6	12	14	28	14	9	27	0	30	61	29 (32.2)
Total	8	0	24	20	20	40	46	92	46	42	126	0	116	238	110 (31.6)
Number of neurons	24			60			138			126			348		

Ed, motor neurons expressing only edited GluR2 mRNA; Uned, motor neurons expressing only unedited GluR2 mRNA. Editing efficiencies of all the specimens from control mice (Ctl1 and Ctl 2; each n = 25) were 100%.

Table S3. Site-selective deamination

Region	Anterior horn		Forebrain	
Editing sites	Control (n = 12)	AR2 (n = 24)	Control (n = 12)	AR2 (n = 12)
Q/R GluR2 mRNA	100 ± 0	84.1 ± 13.0***	99.8 ± 0.3	99.6 ± 0.4
Q/R GluR2 pre-mRNA	100 ± 0	71.9 ± 12.7**	91.2 ± 11.7	93.9 ± 6.6
R/G GluR2 mRNA	94.9 ± 4.9	90.3 ± 5.4	93.7 ± 3.8	94.4 ± 4.9
Q/R GluR5 mRNA	74.7 ± 11.1	79.8 ± 7.4	67.1 ± 13.9	64.1 ± 18.0
Q/R GluR6 mRNA	52.2 ± 20.5 (67.4 ± 15.3) [#]	41.4 ± 31.7 (33.6 ± 31.8*)[#]	90.5 ± 3.2	94.9 ± 3.0
I/V Kv1.1 mRNA	45.1 ± 16.7	45.1 ± 22.1	27.3 ± 12.0	28.5 ± 2 1.4

Numbers are the proportions of edited mRNA to total mRNA (%; mean ± SEM) at each editing site. AR2, ADAR2$^{flox/flox}$/VAChT-Cre.Fast mice; *p = 0.04416; **p = 0.00000025; ***p = 0.00000036 (Mann-Whitney-test); [#], samples from mice older than 5 months of age (control: n = 5; AR2: n = 16).

SUPPLEMENTAL MATERIAL

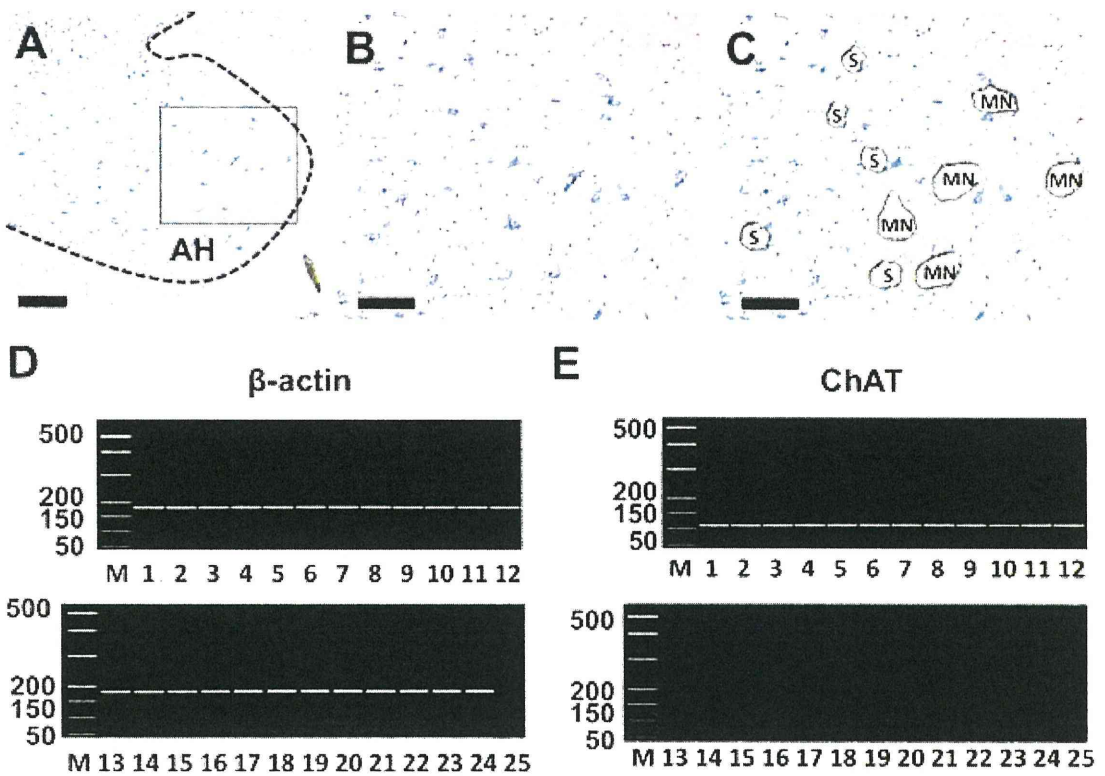

Figure S1. Dissection of motor neurons

A. Spinal cord anterior horn (AH) of AR mice at two months of age was demarcated with dotted line. ***B.*** Magnified view of the boxed region in ***A***, showing large and small neurons in the AH. ***C.*** View of the same region as ***B*** after dissecting large neurons (MN; diameter larger than 20 μm) and small neuron (S; diameter smaller than 19 μm) with a laser microdissector. Sections were stained with 0.1% toluidine blue. ***D, E.*** Gel image of nested RT-PCR for β-actin and choline acetyltransferase (ChAT) on lysates of a single MN (n = 12; lane 1 - 12) and a single S (n = 12; lane 13 - 24), using specific primer pairs (supplemental Table S2, available at www.jneurosci.org as supplemental material). RT-PCR products were analyzed with a Bioanalyzer 2100 (Agilent Technologies). Note that ChAT transcripts were amplified from all the MN lysates but from none of S lysates, indicating that large anterior horn cells (AHCs), but not small anterior horn cells, designated from morphological criteria are motor neurons. Scale bars: 100μm (for ***A***) and 30μm (for ***B*** and ***C***). AH, anterior horn of the spinal cord; M, molecular marker.

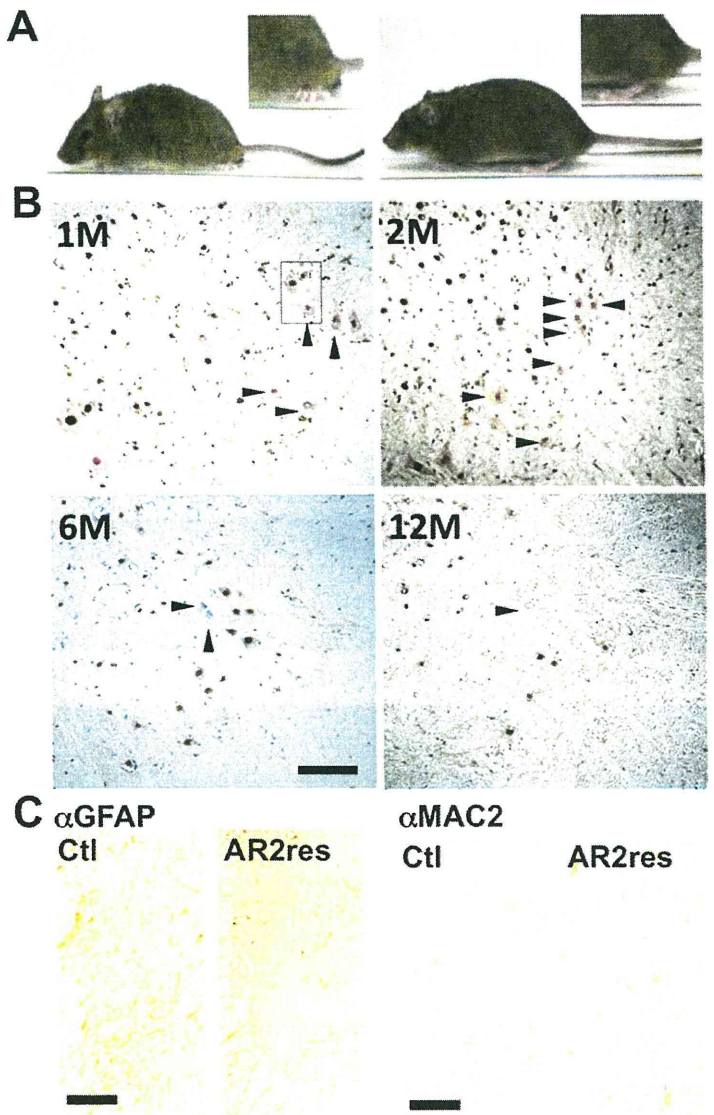

Figure S2. AR2 and AR2res mouse

A. An AR2 mouse at 12 months of age (left panel) exhibits abnormal posture of the hind-limbs and the tail, as compared with normal posture of a control littermate (right panel). ***B.*** Spinal anterior horns of AR2 mice at one (1m), two (2m), six (6m), and 12 months of age (12m). The number of SMI32-positive large anterior horn cells (AHCs) lacking ADAR2-immunoreactivity (arrowheads) decreases with age. Sections were counter-stained with hematoxylin. Scale bar: 100 μm. ***C.*** Immunohistochemistry in the anterior horn of the cervical spinal cord (C5). Consistent with the absence of AHC loss, there is no increase in GFAP- or MAC2-immunoreactivity in the anterior horns of AR2/GluR-$B^{R/R}$ (AR2res) mice as compared to control mice (Ctl) at six months of age. Scale bars: 100μm (left panel) and 50μm (right panel).

Legend for supplemental movie

Spontaneous activity of a 12-month-old AR2 mouse is much lower than that of a littermate wild-type mouse.

Journal of the Neurological Sciences 299 (2010) 126–129

Contents lists available at ScienceDirect

Journal of the Neurological Sciences

journal homepage: www.elsevier.com/locate/jns

Short Communication

Aceruloplasminemia in a Japanese woman with a novel mutation of *CP* gene: Clinical presentations and analysis of genetic and molecular pathogenesis☆

Ayumi Hida [a], Hisatomo Kowa [a,b], Atsushi Iwata [a,b,*], Masaki Tanaka [a], Shin Kwak [a], Shoji Tsuji [a]

[a] Department of Neurology, Graduate School of Medicine, University of Tokyo, 7-3-1 Hongo, Bunkyo-ku, Tokyo 113-8655, Japan
[b] Department of Molecular Neuroscience on Neurodegeneration, Graduate School of Medicine, University of Tokyo, 7-3-1 Hongo, Bunkyo-ku, Tokyo 113-8655, Japan

ARTICLE INFO

Article history:
Received 21 July 2010
Received in revised form 11 August 2010
Accepted 13 August 2010
Available online 15 September 2010

Keywords:
Aceruloplasminemia
Ceruloplasmin
W1017X
Desferrioxamine mesylate

ABSTRACT

We report a Japanese woman diagnosed as aceruloplasminemia showing characteristic symptoms. Mutational analysis of *CP* gene revealed a novel homozygous mutation in exon 18, resulting in prematurely truncated W1017X protein. *In vitro* study showed that W1017X mutant ceruloplasmin was deficient in endoplasmic reticulum to Golgi trafficking and was not secreted to medium. It has been reported that the presence of both the G (FLI/LI) GP domain and the 881th cysteine residue was sufficient for secretion. Thus, our report on this novel mutant indicates the previously unreported importance of carboxy-terminus residues in the secretion pathway.

1. Introduction

Aceruloplasminemia is a rare autosomal recessive disease characterized by diabetes mellitus, retinal degeneration, and various neurological symptoms caused by mutations in the ceruloplasmin (*CP*) gene [1]. Ceruloplasmin is an α2-glycoprotein that carries 95% of plasma copper and plays an essential role in iron metabolism through its ferroxidase activity [2]. The activity is copper dependent, and loss of this activity results in accumulation of iron in the liver, pancreas, retina, and the central nervous system. Iron deposition in brain parenchyma causes ataxia, Parkinsonism, and dementia. The *CP* gene is located in chromosome 3q25, is composed of 20 exons, and has more than 30 previously reported causative mutations [3]. Ceruloplasmin is initially synthesized as a copper-free apo-ceruloplasmin in the endoplasmic reticulum (ER) and is trafficked to the Golgi apparatus to incorporate copper, thus becoming a holo-ceruloplasmin. Functional analysis of the mutant proteins so far revealed two distinctive pathomechanisms. First, copper-binding-deficient mutant apo-ceruloplamins are not functional as ferroxidases and are rapidly degraded in hepatocytes. Secondly, mutants defective in ER to Golgi trafficking are retained in the ER and are not secreted; thus, they lack its function, although they may retain *in vitro* copper-binding ability. The 881st cysteine residue has been reported to be crucial for secretion [4] since the R882X mutant was reported to be successfully secreted into the serum while C881X was not.

Here, we report a 58-year-old woman who was diagnosed as having aceruloplasminemia with a novel *CP* gene mutation resulting to premature truncation at the 1017th tryptophan. This mutant, which is the longest protein among all the carboxy (C)-terminus truncated mutants, showed ER-retention phenotype, indicating that the most C-terminus structure of ceruloplasmin is also crucial for ER to Golgi trafficking.

2. Methods

2.1. MRI images

MRI images were obtained through Siemens Signa HGx (Munich, Germany).

2.2. Genetic analysis

Genetic analysis was performed following written consent from the patient and the caregiver. *CP* gene was amplified using primers published elsewhere [5]. Direct sequence analysis was performed by using the ABI 3700 instrument (Applied Biosystems, Carlsbad, CA, USA).

☆ This study was supported by KAKENHI from JSPS (Japan Society for the Promotion of Science); Japan Ministry of Education, Culture, Sports, Science and Technology; Mochida Memorial Foundation for Medical and Pharmaceutical Research; Brain Science Foundation; Cell Science Research Foundation; and Janssen Pharmaceuticals. AI receives consultant fee from Pfizer Inc. and Bristol Myers, and ST receives consultant fee from Eisai.

* Corresponding author. Department of Molecular Neuroscience on Neurodegeneration, Graduate School of Medicine, University of Tokyo, 7-3-1 Hongo, Bunkyo-ku, Tokyo 113-8655, Japan. Tel.: +81 3 5800 8672; fax: +81 3 5800 6548.
E-mail address: iwata-tky@umin.ac.jp (A. Iwata).

0022-510X/$ – see front matter
doi:10.1016/j.jns.2010.08.019

2.3. Cell culture and immunoblot

Cell culture, immunoblot analysis and microscopic analysis were done as published elsewhere [6]. Ceruloplasmin cDNA was a kind gift from Dr. Kono (Hamamatsu University School of Medicine) [4]. Ceruloplasmin cDNA was subcloned to pcDNA3.1 for expressional analysis. W1017X mutant was made with site directed mutagenesis. Anti-ceruloplasmin antibody was purchased from Bethyl Laboratories (Montgomery, TX, USA), and anti-calreticulin was from Stressgen (Ann Arbor, MI, USA).

3. Results

3.1. Case report

A 58-year-old woman visited our hospital with complaints of cognitive dysfunction, gait instability and neck involuntary movements. At the age of 33, she was diagnosed as having insulin-dependent diabetes mellitus, which had been poorly controlled and was accompanied by frequent hypoglycemia and hyperglycemia that often led to consciousness loss. At the age of 40, she developed hepatitis A, which progressed to severe hepatic dysfunction and coma that required plasmapheresis. At the age of 51, frequent falls began and episodes of memory disturbance emerged. Her cognitive function slowly deteriorated. At the age of 57, neck tremor began. With further deterioration of cognitive function, she became apathetic before the visit to our hospital. Interview on family history revealed that her parents were 1st cousins, and her three siblings died within several months after their birth due to unknown reasons (Fig. 1A).

On neurological examination, she was alert but showed short-term and working memory disturbance, cerebellar ataxia, and 2 to 3 Hz neck tremor which was usually vertical and sometimes horizontal and absent during sleep.

Ophthalmic investigation revealed retinal degeneration without apparent visual impairment. Detailed cognitive function analysis revealed moderate decline in mini-mental state examination (19/30) and marked decline in IQ as measured by WAIS-III (FIQ59, VIQ69, PIQ54). Laboratory findings revealed normal liver enzymes (AST 13 IU/L, ALT 9 IU/L, γGTP 11 IU/L, ALP 271 IU/L); undetectable ceruloplasmin below 2 mg/dL (normal 21–37); increased serum ferritin, 581 ng/mL (4–108); low iron, 21 μg/mL (40–162); copper, 8 μg/mL; transferrin, 163 mg/dL; and decreased urine iron, 0.03 mg/day (normal range 0.1–0.2). Brain magnetic resonance imaging (MRI) revealed diffuse cerebral atrophy and $T2^-$ low signal at the cerebral cortex (Fig. 1B), dentate nucleus (1C) and the basal ganglia (1D). Pulvinar showed high $T2^-$ and low T1 signals bilaterally (1D,E). Abdominal MRI showed that the liver had homogeneously abnormal T2 low intensity (Fig. 1E).

From characteristic MRI findings and the absence of serum ceruloplasmin (Fig. 2A), aceruloplasminemia was suspected. Mutational analysis revealed a novel homozygous non-sense mutation at the exon 18 of the *CP* gene (Fig. 2B), which confirmed the diagnosis. Periodic intramuscular desferrioxamine mesylate was initiated. Cognitive function did not improve after 1 year treatment; however, involuntary movement and gait instability improved.

3.2. Genetic and molecular analysis

The mutation was homozygotic substitution of guanine to adenine that resulted to substitution of tryptophan (tgg) for the stop codon (tag) at the 1017th amino acid, which produced truncated protein that lacks 30 amino acids at its C-terminus. To reveal the pathomechanism

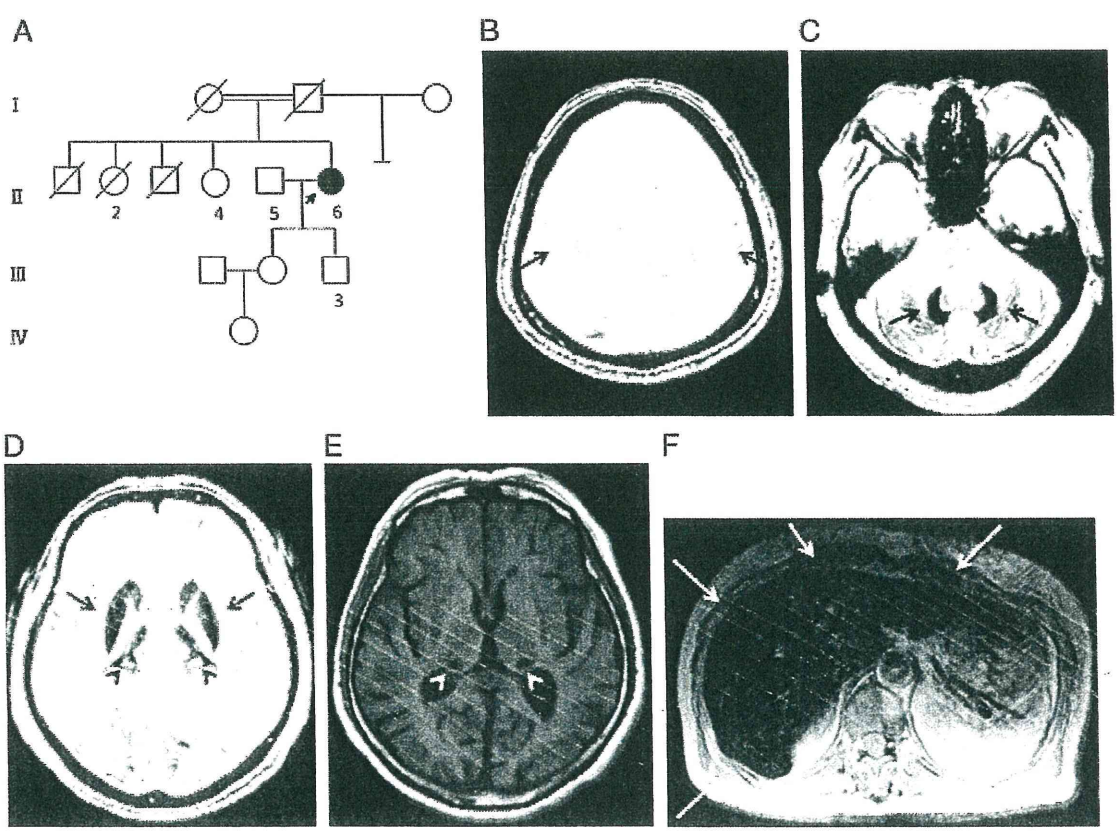

Fig. 1. A: Family tree of the patient. The patient is at II-6, indicated by the arrow. B–E: Magnetic resonance images (MRI) of the brain at the level of the parietal lobe (B: T2), cerebellum (C: T2), and the basal ganglia (D: T2, and E: T1). Arrows indicate abnormal $T2^-$ low intensities. Arrowheads indicate putamen with T2 high and T1 low intensity. F: Abdominal T2-weighted MRI image showing the liver is also abnormally low intensity.

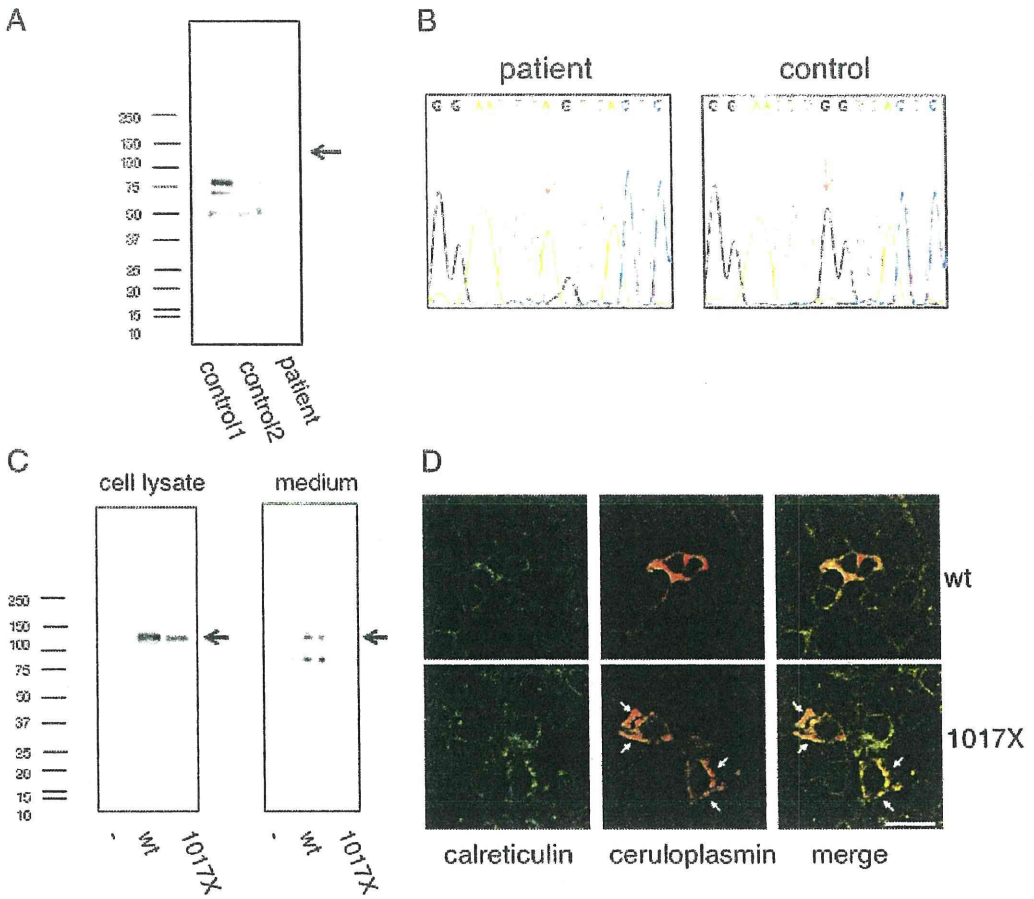

Fig. 2. A. Serum western blot analysis of 2 controls and the patient. Arrow indicates full-length ceruloplasmin. B. Sequence analysis of *CP* gene exon 18. Arrow in the electropherogram of the patient indicates the missense mutation that substitutes tgg (tryptophan) to tag (stop codon). C. Empty plasmid, wild-type ceruloplasmin, and the W1017X mutants were overexpressed in 293T cells. After 48 h of transfection, medium was changed to serum-free medium for 4 h, then the medium and the cells were harvested independently. After cell lysis, both the lysates and the medium were subjected to western blot. Arrows indicate ceruloplasmin. Note that the band in W1017X runs slightly faster than wild type due to the lack of C-terminus 30 amino acids. D. Empty plasmid, wild-type ceruloplasmin, and the W1017X mutants were overexpressed in 293T cells. After 48 h, cells were fixed and stained with anti-calreticulin and anti-ceruloplasmin antibodies. Arrows indicate ceruloplasmin co-localizing with endoplasmic reticulum. Bar = 10 μM.

caused by the W1017X mutation, we transfected wild type or W1017X human CP cDNA to 293T cells. In cell lysates of both wild type and W1017X, the 120-kDa bands corresponding to CP were detected. In the cell culture medium, the band was only detected from wild-type transfected HEK293T and was absent in the medium from the W1017X mutant. This result suggested that the mutant was not capable of secretion. To confirm the result, immunofluorescence microscopy was done. The result clearly showed that the mutant was retained at the ER (Fig. 2D). Thus, we concluded that the W1017X mutant was deficient in extracellular secretion.

4. Discussion

Recent molecular analyses have shown two different mechanisms by which *CP* gene mutations can result to lack of *in vivo* ferroxidase activity [7]. Ceruloplasmin needs two different steps to obtain ferroxidase activity, one is copper incorporation and the other is extracellular secretion by ER to Golgi trafficking. Problems in either step can result to the loss of serum enzyme activity and, thus, accumulation of iron in various tissues. Since the major iron-delivering protein transferrin can only bind to ferric iron, oxidation of ferrous iron (Fe^{2+}) into ferric iron (Fe^{3+}) by ceruloplasmin is required for proper iron transport in the plasma. Although CP may play an important role in normal brain iron metabolism, circulating CP cannot cross the blood–brain barrier. Thus, in the central nervous system, CP is expressed on the surface of astrocytes as the glycosylphosphatidylinositol (GPI)-anchored form. The GPI-anchored form is generated by alternative RNA splicing that occurs downstream of exon 18 and replaces the C-terminal 5 amino acids of the secreted form with alternative 30 amino acids [8,9]. Since the mutation found in this patient is an early truncation at exon 18, the GPI-anchored form is also expected to be non-functional.

Our molecular analysis revealed that the W1017X mutant protein was not secreted to the medium. Microscopic images also show co-localization of W1017X mutant with the ER, while wild type shows wide distribution in the cytoplasm. These results suggest that the W1017X mutant protein is improperly retained in the ER, which results to loss of serum ferroxidase activity. Since the copper-binding histidine residues are located throughout the protein and the most C-terminus one is located after the mutation site, it is still possible that the W1017X mutant still lacks the full ferroxidase activity [10]. To our knowledge, this W1017X mutant is the longest truncated mutant CP among all the reports.

In human CP, the G (FLI/LI) CP motif is repeated 6 times and is conserved in the homologous proteins hephaestin and factor VIII. Proline residue in the motif has been shown to be crucial for intracellular trafficking; therefore the motif had been thought to have an important role in packing hydrophobic side chain, protein folding, and assembly in the ER [7,11]. In a recent study, truncated mutant CP that lacks the 881st cysteine residue was unable to undergo trafficking [4]. This result suggested that the residue was essential for the secretion, possibly by forming a disulfide bond with the 855th cysteine.

Our study suggests that the downstream residues of the 1017th tryptophan near the C-terminal are also necessary for GP secretion in addition to previously reported 6 C (FU LI) GP domains of Cys-881 residue. The patient's brain and liver MRI clearly indicates that the patient has iron metabolism disorder across the brain-blood barrier; thus, it is unlikely that the W1017X mutant is pathogenic only as a GPI-anchored form. Since the C-terminus of ceruloplasmin contains hydrophobic residues, the C-terminus tertiary structure of the protein could be important for its secretion.

Magnetic resonance imaging is indispensable for demonstrating iron deposition. In the present case, typical abnormalities were observed in the basal ganglia and dentate nucleus. In addition, bilateral pulvinar showed T2 high and T1 low intensity area surrounded by T2 low and T1 low intensities suggesting that the central pulvinar was cavitated. One possibility is that this case is so advanced that cystic degeneration might have developed [12]. Alternatively, her past history of hepatic coma at age 40 might have influenced to those intensity changes of bilateral thalamus [13,14], although she showed no neurological symptoms right after the episode.

Several studies have reported treating aceruloplasminemia with ion-chelating agents such as desferrioxamine mesylate [15]. Desferrioxamine is a high-affinity iron chelator binding with ferric ion, and promotes the excretion of excess and potentially toxic iron in patients with iron overload [15]. Some cases treated with zinc sulfate to reduce iron-related oxidative stress showed neurological improvement to a certain extent [16]. In our case, after 1 year of intramuscular desferrioxamine, the patient's cognitive impairment did not change, but the amplitude of the neck tremor and gait instability improved suggesting that the iron chelation could be beneficial for the patent. Recently, deferasirox, also an iron chelator, was reported to be effective for aceruloplasminemia [3]. The use of this drug could be an option for this patient in the future.

Contributors

1. Research project: A. conception, B. organization, and C. execution.
2. Manuscript: A. writing of the first draft, and B. review and critique.

AH 1A, 1B, 1C, 2A; HK 1A, 1B, 2B; AI 1A, 1B, 1C, 2A; MT 1C; SK 2B; ST 1A, 2B.

Acknowledgment

We thank Dr. Satoshi Kono (First Department of Medicine, Hamamatsu University School of Medicine) for the GP-cDNA.

References

[1] Miyajima H, Nishimura Y, Mizoguchi K, Sakamoto M, Shimizu T, Honda N. Familial apoceruloplasmin deficiency associated with blepharospasm and retinal degeneration. Neurology 1987;37(5):761–7.
[2] Miyajima H, Takahashi Y, Kono S. Aceruloplasminemia, an inherited disorder of iron metabolism. Biometals 2003;16(1):205–13.
[3] McNeill A, Pandolfo M, Kuhn J, Shang H, Miyajima H. The neurological presentation of ceruloplasmin gene mutations. Eur Neurol 2008;60(4):200–5.
[4] Kono S, Suzuki H, Oda T, Shirakawa K, Takahashi Y, Kitagawa M, et al. Cys-881 is essential for the trafficking and secretion of truncated mutant ceruloplasmin in aceruloplasminemia. J Hepatol 2007;47(6):844–50.
[5] Harris ZL, Takahashi Y, Miyajima H, Serizawa M, MacGillivray RT, Gitlin JD. Aceruloplasminemia: molecular characterization of this disorder of iron metabolism. Proc Natl Acad Sci USA 1995;92(7):2539–43.
[6] Iwata A, Nagashima Y, Matsumoto L, Suzuki T, Yamanaka T, Date H, et al. Intranuclear degradation of polyglutamine aggregates by the ubiquitin-proteasome system. J Biol Chem 2009;284(15):9796–803.
[7] Kono S, Miyajima H. Molecular and pathological basis of aceruloplasminemia. Biol Res 2006;39(1):15–23.
[8] Patel BN, Dunn RJ, David S. Alternative RNA splicing generates a glycosylphosphatidylinositol-anchored form of ceruloplasmin in mammalian brain. J Biol Chem 2000;275(6):4305–10.
[9] Vasiliev V, Harris ZL, Zatta P. Ceruloplasmin in neurodegenerative diseases. Brain Res Brain Res Rev 2005;49(3):633–40.
[10] Hellman NE, Kono S, Mancini GM, Hoogeboom AJ, De Jong GJ, Gitlin JD. Mechanisms of copper incorporation into human ceruloplasmin. J Biol Chem 2002;277(48):46632–8.
[11] Hellman NE, Kono S, Miyajima H, Gitlin JD. Biochemical analysis of a missense mutation in aceruloplasminemia. J Biol Chem 2002;277(2):1375–80.
[12] McNeill A, Birchall D, Hayflick SJ, Gregory A, Schenk JF, Zimmerman EA, et al. T2 and FSE MRI distinguishes four subtypes of neurodegeneration with brain iron accumulation. Neurology 2008;70(18):1614–9.
[13] Fridman V, Galetta SL, Pruitt AA, Levine JM. MRI findings associated with acute liver failure. Neurology 2009;72(24):2130–1.
[14] McKinney AM, Lohman BD, Sarikaya B, Uhlmann E, Spanbauer J, Singewald T, et al. Acute hepatic encephalopathy: diffusion-weighted and fluid-attenuated inversion recovery findings, and correlation with plasma ammonia level and clinical outcome. AJNR Am J Neuroradiol 2010. doi:10.3174/ajnr.A2112.
[15] Miyajima H, Takahashi Y, Kamata T, Shimizu H, Sakai N, Gitlin JD. Use of desferrioxamine in the treatment of aceruloplasminemia. Ann Neurol 1997;41(3):404–7.
[16] Kuhn J, Miyajima H, Takahashi Y, Kunath B, Hartmann-Klosterkoetter U, Cooper-Mahkorn D, et al. Extrapyramidal and cerebellar movement disorder in association with heterozygous ceruloplasmin gene mutation. J Neurol 2005;252(1):111–3

Lesion of the Nucleus Intercalatus in Primary Position Upbeat Nystagmus

A 32-YEAR-OLD WOMAN was admitted to our hospital with dizziness lasting 2 weeks. On neurological examination, she showed primary position upbeat nystagmus (**Figure 1**; video, http://www.archneurol.com). There were no other neurological abnormalities. T2-weighted magnetic resonance and fluid-attenuated inversion recovery imaging revealed multiple periventricular white matter lesions in the brain. A high-intensity spot was also present in the left side of posterior caudal medulla (Figure 1). We diagnosed her with multiple sclerosis and started 1 mg/d of methylprednisolone pulse therapy for 3 days. She gradually recovered, and the symptom disappeared in 2 weeks. The abnormal lesion in the medulla also became undetectable on magnetic resonance imaging.

Video available online at www.archneurol.com

COMMENT

Primary position upbeat nystagmus (PPUN) is an upward vertical nystagmus that is rarely observed in brainstem disorders. The lesion responsible for PPUN was considered to be in either the ventral tegmental tract in pons or caudal medulla. To date, PPUN has been reported in 3 cases with medullary lesions.[1-3] The lesion in our case was localized in the overlapped region described in 2 articles by Munro et al[1] and Hirose et al.[2] The lesion in our case was confined to an extremely small area of part of the most dorsal medulla, and its location corresponded to the location of the nucleus intercalatus according to several microscopic anatomical charts. The lesion in the present case was located in a more dorsal portion of the medulla than those described by Munro et al[1] and Hirose et al.[2] Therefore, our case seems to be the most convincing evidence to date that a lesion of the intercalatus nucleus is a candidate for PPUN. Janssen et al[3] also described a case with PPUN. His lesion existed in the dorsal paramedial caudal medulla, which encompassed the nucleus intercalatus. Pierrot-Deseilligny and Milea[4] illustrated the neural circuit and explained why a lesion in the posterior caudal medulla produces primary position upbeat nystagmus (**Figure 2**). When the nucleus intercalatus is invaded, the superior rectus responds with impaired functioning and, eventually, the eyeball continually moves downward. Consequently, upbeat nystagmus appears. To confirm the lesion in the medulla responsible for PPUN, accumulation of similar cases is needed.

Tsukasa Saito, MD
Hitoshi Aizawa, MD, PhD
Jun Sawada, MD, PhD
Takayuki Katayama, MD, PhD
Naoyuki Hasebe, MD, PhD

Accepted for Publication: February 9, 2010.
Correspondence: Dr Saito, Division of Neurology, Department of Internal Medicine, Asahikawa Medical College, Asahikawa, Hokkaido 078-8510, Japan (tsukasa@asahikawa-med.ac.jp).
Author Contributions: *Study concept and design*: Saito, Aizawa, and Hasebe. *Acquisition of data*: Saito and Sawada. *Analysis and interpretation of data*: Saito, Aizawa, and Katayama. *Drafting of the manuscript*: Saito. *Critical revision of the manuscript for important intellectual content*: Saito, Aizawa, Sawada, Katayama, and Hasebe. *Administrative, technical, or material support*: Katayama. *Study supervision*: Aizawa, Katayama, and Hasebe.
Financial Disclosure: None reported.
Online-only Material: A video is available at http://www.archneurol.com.

REFERENCES

1. Munro NAR, Gaymard B, Rivaud S, Majdalani A, Pierrot-Deseilligny C. Upbeat nystagmus in a patient with a small medullary infarct. *J Neurol Neurosurg Psychiatry.* 1993;56(10):1126-1128.
2. Hirose G, Ogasawara T, Shirakawa T, et al. Primary position upbeat nystagmus due to unilateral medial medullary infarction. *Ann Neurol.* 1998; 43(3):403-406.
3. Janssen JC, Larner AJ, Morris H, Bronstein AM, Farmer SF. Upbeat nystagmus: clinicoanatomical correlation. *J Neurol Neurosurg Psychiatry.* 1998; 65(3):380-381.
4. Pierrot-Deseilligny C, Milea D. Vertical nystagmus: clinical facts and hypotheses. *Brain.* 2005; 128(pt 6):1237-1246.

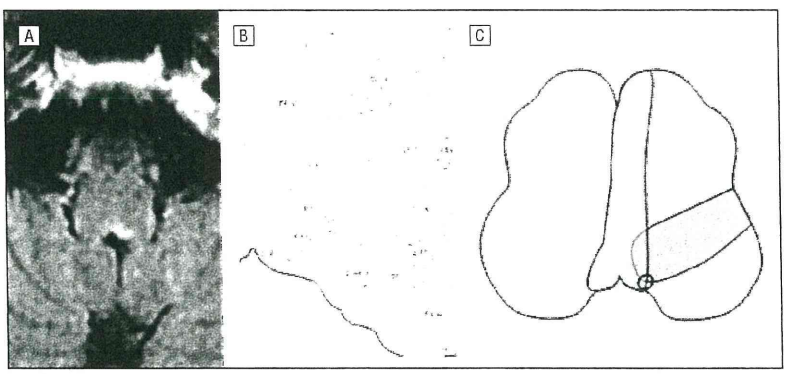

Figure 1. The lesion, presenting on the left side of the dorsal caudal medulla. Part B is taken from Olszewski J, Baxter D. *Cytoarchitecture of the Human Brain Stem.* 2nd ed. Basel, NY: Karger; 1982.

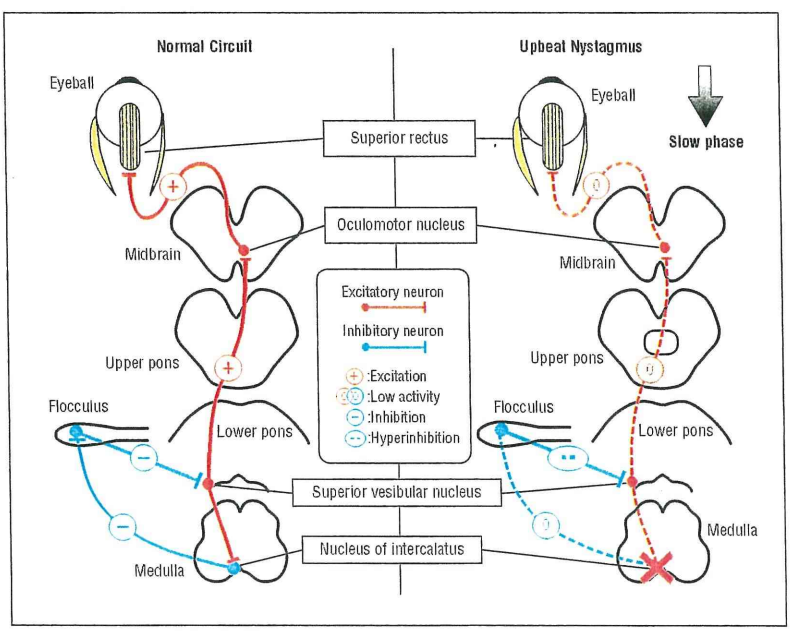

Figure 2. Schematic diagram. Modified with permission from *Brain*.[4]

OBSERVATION

Anti–*N*-methyl-D-aspartate Receptor Encephalitis During Pregnancy

Monisha A. Kumar, MD; Ankit Jain, BS; Valerie E. Dechant, MD; Tsukasa Saito, MD; Timothy Rafael, MD; Hitoshi Aizawa, MD, PhD; Kevin C. Dysart, MD; Takayuki Katayama, MD, PhD; Yasuo Ito, MD; Nobuo Araki, MD; Tatsuya Abe, MD; Rita Balice-Gordon, PhD; Josep Dalmau, MD, PhD

Objective: To report 3 patients who developed anti–*N*-methyl-D-aspartate receptor encephalitis during pregnancy.

Design: Case reports.

Setting: University hospitals.

Patients: Three young women developed at 14, 8, and 17 weeks of gestation acute change of behavior, prominent psychiatric symptoms, progressive decrease of consciousness, seizures, dyskinesias, and autonomic dysfunction.

Main Outcome Measures: Clinical, radiological, and immunological findings.

Results: The 3 patients had cerebrospinal fluid pleocytosis, normal magnetic resonance imaging, and electroencephalogram showing slow activity. All had higher antibody titers in cerebrospinal fluid than in serum and 2 had ovarian teratomas that were removed. The pregnancy was terminated in 1 patient with recurrent bilateral teratomas. All patients had substantial neurological recoveries, and the 2 newborns were normal. Results of extensive antibody testing in 1 of the babies were negative.

Conclusion: The current study shows that anti-NMDAR encephalitis during pregnancy can have a good outcome for the mother and newborn.

Arch Neurol. 2010;67(7):884-887.

Author Affiliations: Departments of Neurology (Drs Kumar and Dechant), Obstetrics and Gynecology (Dr Rafael), and Pediatrics (Dr Dysart), Thomas Jefferson University Hospital, and Departments of Neuroscience (Mr Jain and Dr Balice-Gordon) and Neurology (Dr Dalmau), University of Pennsylvania, School of Medicine, Philadelphia; and Division of Neurology, Department of Internal Medicine, Asahikawa Medical College, Asahikawa, Hokkaido (Drs Saito, Aizawa, and Katayama) and Division of Neurology, School of Medicine, Saitama Medical University, Moroyama, Saitama (Drs Ito, Araki, and Abe), Japan.

Anti–*N*-methyl-D-aspartate receptor (NMDAR) encephalitis is a synaptic autoimmune disorder that is likely mediated by antibodies against the NR1 subunit of the receptor.[1] Despite the severity of the disorder, most patients have substantial recoveries. Because the disease frequently affects women of childbearing age and the antibody subtypes (IgG1, IgG3) can cross the placenta, there is concern about the effects of the disorder during pregnancy.[2] We report 3 patients who developed the disorder during pregnancy.

REPORT OF CASES

Clinical features from the patients are described in this section and summarized in the **Table**. Antibodies to NMDAR were detected as reported elsewhere[1] and the titers were determined by serial dilution (starting at 1:10). The baby of patient 1 had antibody studies in the umbilical cord, serum, cerebrospinal fluid (CSF), and amniotic fluid.

CASE 1

A 19-year-old woman presented at 14 weeks of gestation with 2 weeks of headache and malaise followed by bizarre behavior and paranoid delusions resulting in hospitalization. Over the course of a week, her mental status worsened until she was minimally responsive. She had a generalized seizure that was treated with fosphenytoin and lorazepam, and she was intubated for airway protection. A bedside electroencephalogram (EEG) revealed generalized slowing but no epileptic activity. On examination, she was minimally responsive to noxious stimuli, had generalized hyperreflexia, and moved all limbs spontaneously. Results of magnetic resonance imaging (MRI) and CSF studies are described in the Table. Treatment with acyclovir was started for presumptive viral encephalitis.

On the third day in the intensive care unit, she developed repetitive pursing of the lips and furrowing of her brow without EEG correlates. These movements became more frequent and the dyskinesias spread to her limbs. By day 8, she developed diaphoresis, tachycardia, mydriasis, and hypertension. These symptoms were difficult to control despite treatment with fentanyl, lorazepam, propofol, bromocriptine, and β-blockers.

On day 5, a tracheostomy was performed. Treatment with intravenous immunoglobulin did not result in improvement. On day 23, an MRI of the abdomen and pelvis revealed a 2.5×3-cm left ovarian simple cyst. On day 43, NMDAR antibodies were identified in CSF. A second course of intravenous immunoglobulin treatment along with 1 g of methylprednisolone was given daily for 5 days. On day 50,

Table. Clinical Information and Antibody Titers

Patient	First Symptom of Encephalitis During Pregnancy	Other Symptoms	Teratoma	EEG	CSF WBC Count, /μL[a]	Week of Pregnancy, Antibody Titers in Serum and CSF	Outcome[b]
1	14th wk: Headache, malaise, bizarre behavior	Seizure, orofacial and limb dyskinesias, autonomic instability, minimally responsive	Left immature teratoma	Slow activity	244	14th wk: serum, ND; CSF, 1:80; 21st wk: serum, ND; CSF, 1:10; 32nd week: serum, ND; CSF, ND; baby at birth: serum, CSF, and umbilical cord blood, ND	Cesarean section at week 38; healthy baby; home on day 184; substantial recovery at 2-mo follow-up
2	8th wk: Abnormal, stereotyped behavior	Orofacial dyskinesias, autonomic dysfunction, seizures, minimally responsive, respiratory depression	Bilateral mature teratomas	1-Hz spikes, slow activity predominantly in frontal lobes	57	10th wk: serum, ND; CSF, 1:320; 13th week: serum, ND; CSF, 1:40	Bilateral tumor removal; pregnancy terminated; right ovary left to preserve fertility; home with minimal deficits on day 87
3	17th wk: Affective and behavioral change	Orofacial movements, tonic seizure without EEG correlate, episodes of agitation alternating with minimal response	No tumor or cyst	Generalized high-amplitude slow activity, 2 Hz	11	19th wk: serum, 1:320; CSF, 1:640; 5 mo postdelivery: serum, 1:80; CSF, NA	Spontaneous delivery at 37 wk of pregnancy; healthy baby; home 23 wk after symptom presentation; full recovery at last follow-up

Abbreviations: CSF, cerebrospinal fluid; EEG, electroencephalogram; NA, not applicable; ND, not detectable (<1:10); NMDAR, *N*-methyl-D-aspartate receptor; WBC, white blood cell.

[a] Normal, ≤4/μL. All 3 patients had normal CSF protein and glucose concentrations.

[b] Days relate to duration of stay in the hospital.

a left oophorectomy was performed, revealing an immature teratoma. On day 52, plasmapheresis was initiated, with a total of 7 treatments over 2 weeks. On day 72, she became more alert, responded to voice, and tracked objects. Throughout the hospitalization, the fetus was monitored weekly by Doppler ultrasonography, showing normal heart tones. Obstetric ultrasonography performed at weeks 20 and 26 revealed normal fetal anatomy and appropriate growth for gestational age.

The patient remained in the intensive care unit because of persistence of sympathetic storms. By day 107, she was following simple commands and the sedation was slowly weaned. On day 127, she began mouthing words. A cesarean section and concomitant surgical staging was performed on day 166 (at 37 weeks of gestation, following amniocentesis confirming fetal lung maturity). The infant weighted 6 lb 3 oz and Apgar scores were 3 at 1 minute and 6 at 5 minutes. All pathological specimens (left adnexa, pelvic lymph nodes, and peritoneal samples) were negative for tumor. Over the next 3 days, the patient was weaned from the ventilator and she made steady gains in physical therapy. By day 184, she was able to ambulate with a walker and her speech was fluent, but she was only oriented to self. Her progress was hampered by impulsivity, short-term memory loss, and physical deconditioning. Two months after discharge, she was functioning independently at home, although she was persistently impulsive and complained of somnolence. The infant has met all developmental milestones to date.

CASE 2

A 20-year-old woman developed change of behavior during the eighth week of pregnancy. She became argumentative, refused to talk and eat, and developed stereotyped behaviors, such as walking endlessly around a room or filling and emptying a glass with water. Two days before hospital admission, semirhythmic movements including blinking, licking, and tongue protrusion were noted. One day before admission, she developed hyperthermia and decreased level of consciousness and had a seizure. She had a history of bilateral ovarian teratomas that were removed when she was 16 years of age.

At admission, she had neck stiffness, without fever, and showed repetitive orofacial movements. She was poorly responsive to verbal and painful stimuli and had generalized hyperreflexia. Ancillary test results are described in the Table. Intravenous acyclovir and methylprednisolone administration were started. On day 3, cardiac pauses up to 5 seconds were noted (**Figure**, A). Over the next few days, she developed hypersalivation and generalized tonic convulsions. On day 13, status epilepticus and respiratory depression led to intubation and mechanical ventilation. On day 15, a pelvic computed tomographic scan revealed bilateral ovarian tumors (Figure, B, arrows); 2 days later, a left salpingo-oophorectomy and removal of both tumors was performed, and the pregnancy was terminated. Pathological studies confirmed bilateral mature teratomas.

From days 23 to 27, she received intravenous immunoglobulin and sedation with midazolam was discontinued. She gradually started tracking objects and following commands but continued having partial seizures that were treated with carbamazepine and gabapentin. On days 32 to 36, intravenous immunoglobulin administration was repeated, and by day 43, she was able to breathe spontaneously. By day 52, she was able to drink; the last seizure was observed on day 53. On day 64, she was eating regularly, and a few days later, she was able to walk. Her Mini-Mental State Examination score was 27 of 30 on day 85 and she was discharged home with minimal deficits on day 87.

CASE 3

A 19-year-old pregnant woman presented at 17 weeks of gestation with acute-onset behavioral change, including increas-